Available online at www.sciencedirect.com

ScienceDirect

Procedia Engineering 199 (2017) 3450–3455

Procedia Engineering

www.elsevier.com/locate/procedia

International Conference on Structural Dynamics, EURODYN 2017

Investigation of Oscillating-Foil Power Generation in Constrained Flow

C.M. Hoke[a,*], J. Young[b], J.C.S. Lai[c], F. Karakas[d], B. Zaloglu[e], I. Fenercioglu[f]

[a]Lecturer, The University of New South Wales Canberra, Canberra, ACT 2600, Australia
[b]Assistant Professor, The University of New South Wales Canberra, Canberra, ACT 2600, Australia
[c]Professor, The University of New South Wales Canberra, Canberra, ACT 2600, Australia
[d]MSc Student, Istanbul Technical University, 34469, Turkey
[e]PhD Student, Istanbul Technical University, 34469, Turkey
[f]Postdoc Researcher/Lecturer, Istanbul Technical University, 34469, Turkey

Abstract

This paper presents a numerical study of a 2D pitching and plunging flat plate foil operating in the vicinity of near side walls. The effects of the side wall proximity and the stroke reversal fraction are compared to previously published water tunnel experimental results and the resulting vortex structures are used to comment on the effect of the constrained flow on overall power generation. Three side wall distances are defined by the closest approach of the trailing edge of the foil during the flapping cycle, including $d_w = 0.1c$, $d_w = 0.5c$, and $d_w = 1.0c$ as well as 'Free Flow' case done with tunnel walls at a distance of $10.0c$. The stroke reversal fraction determines how quickly the foil pitches at the top and bottom of each flapping stroke and varies in increments of 0.1 from $\Delta T_R = 0.1$ to $\Delta T_R = 0.5$ (the sinusoidal pitching case). The foil pivots about its 0.44 chord point and has a plunge amplitude of $1.05c$, a phase angle between pitch and plunge of $\phi = 90°$, and a pitching amplitude of 73°. All cases are run at a Reynolds Number of 10,000 and a non dimensional frequency of $k = 0.8$. The flow solver is Fluent v14.5, run with second order spatial discretization and first order time stepping using a dynamically layered mesh to plunge the airfoil. Grid refinement and turbulence model studies are performed. The results are compared to previously published water tunnel experiments that use direct force measurements as well as PIV to visualize the flow patterns. Overall, the effect of the side walls is small compared to the effect of the reversal fraction or kinematic parameters, however it is demonstrated that the lift on the foil is increased near the wall due to an increase of the local velocity over the foil as the wall distance decreases. However, this changes the positions of the vortices during the rest of the flapping cycle and may or may not increase the overall efficiency depending on the choice of kinematic parameters. The highest increase in efficiency occurs for the sinusoidal motion ($\Delta T_R = 0.5$) at a wall distance of $d_w = 0.5$, in which the overall power extraction efficiency increases to $\eta = 14.2\%$ as compared to the free flow efficiency of $\eta = 11.1\%$, a relative increase of 28%. These trends are similar to those shown by the previously published experimental results.

© 2017 The Authors. Published by Elsevier Ltd.
Peer-review under responsibility of the organizing committee of EURODYN 2017.

Keywords: Oscillating Foil; Flapping Wing; Power Generation; PIV; Constrained Flow; Low Reynolds Number; CFD

* Corresponding author. Tel.: +61 2 6268 8209
E-mail address: c.hoke@adfa.edu.au

1877-7058 © 2017 The Authors. Published by Elsevier Ltd.
Peer-review under responsibility of the organizing committee of EURODYN 2017.
10.1016/j.proeng.2017.09.450

1. Introduction

Considering possible augmentations in power generation near solid wall proximities, the aim of this study is to numerically investigate the power extraction performance of a non-sinusoidally oscillating rectangular foil in 2D free and constrained flows using two side walls placed at various distances from the flat plate. The potential applications are for a sailing ship based renewable energy generator where the wall inserts simulate the hull of a catamaran-type sailing ship with the flapping foil operating underwater, or a turbine in an irrigation channel. The parameters considered in this study are: Reynolds number $Re = 10,000$, non-dimensional plunge amplitude to chord ratio $h = 1.05$, pitch motion amplitude $\theta_0 = 73°$, a phase angle between pitch and plunge of $\phi = 90°$, stroke reversal times ΔT_R of 0.1 (rapid reversal) to 0.5 (sinusoidal reversal) and pitch pivot location $s_{piv} = 0.44$ from the leading edge. The non-dimensional distance between the two side wall inserts are chosen as $h_w = 340, 420$, and $520mm$, corresponding to non-dimensional wall distances from the closest approach of the trailing edge of $d_w = 0.1, 0.5$, and $1.0c$. The computational solutions are run on the commercially available Fluent 14.5 flow solver with a dynamically layered mesh to simulate the plunging airfoil within the water tunnel walls. The results are then compared with previously published experimental results by the authors[1], [2].

2. Methods

2.1. Numerical Setup

Numerical simulations were performed in 2D using the commercial CFD solver Fluent 14.5. The unsteady incompressible Navier Stokes equations were solved with SIMPLE second order spatial discretizations for pressure and momentum and first order time stepping, which is a limitation in Fluent when using a deforming mesh. All calculations with flow conditions matching the experimental setup were done at a Reynolds Number of 10,000. Consistent with earlier studies of flapping foils in these Reynolds number ranges[3], 1,280 time steps were used per flapping cycle and all solutions were run a minimum of 8 flapping cycles to eliminate any startup transients and establish a repeating cycle to cycle consistency. The mesh consists of a rotating circular unstructured zone embedded in a 'piston' zone that translates as the foil plunges, and dynamically re-layers the mesh above and below up to the lower and upper boundaries, corresponding to the walls of the experimental water tunnel. Grid refinement and turbulence model studies were performed, and the $k - \omega$ SST was selected for the remainder of this study due to its close match with experimental visualizations of the shed vortex locations.

2.1.1. Kinematics

The kinematic motion of the flat plate is a combined plunging and pitching motion, with non-sinusoidal pitching and plunging for reversal fractions less than 0.5, where as the reversal fraction decreases the pitching reversals become more rapid. The motion of the flat plate consists of a period of constant translational velocity combined with a constant pitch angle (the 'plunging maneuver'), followed by a sinusoidal reversal of direction and pitch angle (the 'pitching maneuver'). The motion goverened by the stroke reversal time $\Delta T_R = 0.1$, expressed as a fraction of the total cycle, and ranges from $\Delta T_R = 0.1$ for rapid reversal to $\Delta T_R = 0.5$ for purely sinusoidal motion.

The non-dimensional plunge motion amplitude h is 1.05 and the pitch motion amplitude θ_0 is 73° as consistent with previous studies [4,5]. The reduced frequency (k) is defined as $k = \frac{2\pi fc}{U_\infty}$, and set constant at $k = 0.8$ throughout this study. The Reynolds number considered for this study is Re = 10,000 with the corresponding flapping frequency of $f = 0.125$ Hz. The flat plate undergoes combined non-sinusoidal pitching and plunging oscillations with a phase difference $\phi = 90°$, where the pitch leads the plunge motion.

A previous numerical and experimental study [4] shows a marked advantage in changing the pitch pivot location from quarter chord point to mid-chord location. In other numerical studies for a sinusoidally oscillating hydropower generator, 0.44 - 0.46 chord pivot locations [6] were considered ideal while optimum power generation was reported when the pivot location of a flapping foil was positioned between 0.33c and

0.5c from the leading edge[7] in free flow. The test model of the oscillating-wing power generator also relies on two control rods placed at 44% chord to reverse the wing's translatory motion[8]. Thus, the pitch pivot location is set to 0.44 chord position in this study ($s_{piv} = 0.44$).

A small correction had to be made in the computational solution to smooth out a discontinuity in the rotational acceleration that manifests in the equations of motion for the foil, that was unnoticed in the experiment due to the natural damping inherant in any real system. A 7th order polynomial function in the rotational position was used that enforced position, first, and second derivative boundary condition matching at the start and the end of the plunging maneuver as well as the first derivative at the midpoint of the maneuver.

2.2. Experimental Setup

The experimental results cited in this paper have been previously published[1]. The experiments are performed in the closed-circuit, large scale water channel located in the Trisonic Laboratories at the Faculty of Aeronautics and Astronautics of Istanbul Technical University.

3. Results

3.1. Overview of Flapping Cycle Vortex Patterns

A flapping foil power generation system produces power by utilizing the strong leading edge vortex (LEV) caused by high pitching angles to produce lift during the plunging stroke, resulting in translational power (Cp_y) and then rotating through the pitching maneuver when that LEV has translated to the rear of the foil so that it can assist in the pitching maneuver and generate additional power (Cp_θ). The reversal fraction has a large effect on the overall efficiency, as a lower reversal fraction means that the pitching maneuver happens much faster, and therefore the Cp_θ term often dominates the power extraction. Figure 1 shows the vorticity patterns for half of a flapping cycle, in this example for the sinusoidal case ($\Delta T_R = 0.5$). The strong LEV is clearly seen during the translational portion of the cycle and its proximity to the foil surface determines the amount of lift generated. For these conditions, a secondary vortex is induced on the surface of the foil, clearly shown at $t/T = 2/16$. There is also a clear trailing edge vortex (TEV) present at $t/T = 3/16$ forming at the rear of the foil which will have an effect on the pitching efficiency. Some wall interaction is also visible as the vortices induce secondary structures due to the close proximity of the side wall. Figure 2

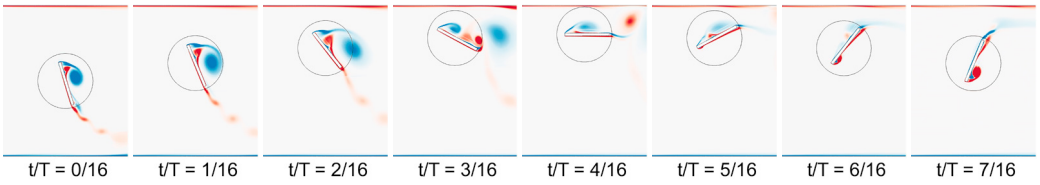

Fig. 1. Visualization of a flapping cycle ($\Delta T_R = 0.5$, $d_w = 0.1$, $\phi = 90°$)

shows the fast reversal fraction cycle ($\Delta T_R = 0.1$). For these conditions, this case does not produce a positive overall power output, although in other studies a faster reversal fraction can result in high efficiencies [7], but the same principles apply - a strong LEV in the vicinity of the airfoil during the plunging stroke and the interaction of the TE with both the LEV and TEV are key to the production of power. For these conditions, it is clear that the high average pitching angles during the plunging stroke result in the formation of two separate LEV during each half-cycle; the first can be seen already well detached from the foil at $t/T = 0/16$ while the second is formed just prior to the pitching maneuver at $t/T = 3/16$. The pitch maneuver itself is quite fast and produces another opposite sense vortex on the leeward side of the airfoil just after the

pitching maneuver, as can be visualized at $t/T = 5/16$. The effect of the wall is also quite clearly seen, with two secondary vortices visible at $t/T = 6/16$. As mentioned, the overall effect of all these interactions results in negative power generation for this particular set of flow conditions.

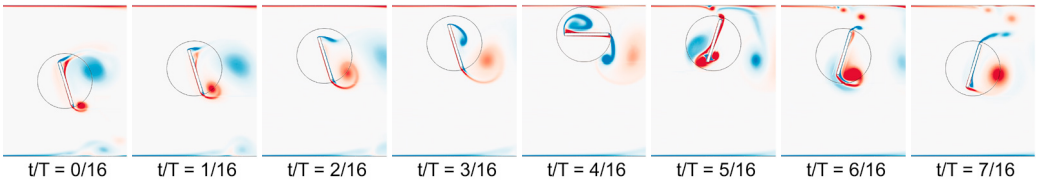

Fig. 2. Visualization of a flapping cycle ($\Delta T_R = 0.1$, $d_w = 0.1$, $\phi = 90°$)

3.2. Effect of Wall Distance on Aerodynamic and Power Extraction Coefficients

For the flow conditions presented in this paper, the sinusoidal reversal fraction ($\Delta T_R = 0.5$) produces the highest overall efficiencies, as shown in Figure 3. The power extraction efficiency is much more sensitive to the reversal fraction than the wall distance overall, and the effect of the wall varies depending on the reversal fraction. For the quicker reversal fractions $\Delta T_R = 0.1$ to $\Delta T_R = 0.3$, as the wall moves closer to the foil the efficiency decreases, particularly at the closest wall distance ($d_w = 0.1$). However, for the slower reversal fractions of $\Delta T_R = 0.4$ and $\Delta T_R = 0.5$, the wall can increase the efficiencies, most noticeably at $d_w = 1.0$ for $\Delta T_R = 0.4$ and at $d_w = 0.5$ for the sinusoidal case, $\Delta T_R = 0.5$. In the latter case, the power extraction efficiency increases from $\eta = 11.1\%$ in the freestream case to $\eta = 14.2\%$, a relative increase of 28%. The effect

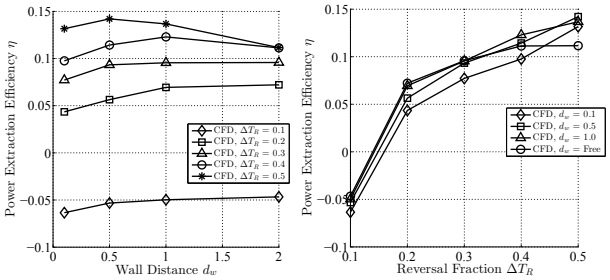

Fig. 3. Power Extraction Efficiency a) As a Function of Wall Distance b) As a Function of Reversal Fraction

of the wall can be seen in the resulting power extraction coefficients as shown in Figure 4. The most obvious effect is an increase in the lift coefficient as the wall distance decreases, which manifests as a clear increase in the power extraction due to the vertical plunging motion, Cp_y. The peak of Cp_y during the plunging strokes (at $t/T = 0/16$, $8/16$, and $16/16$) increases from approximately 0.4 in the freestream cases to 0.6 at $d_w = 0.1$, nearly a 50% increase. However, as mentioned earlier, the overall max efficiency increase occurs at $d_w = 0.5$ for this reversal fraction, and this is due to the fact that the negative contributions before and during $t/T = 4/16$ are not as pronounced in that case. This lift increase occurs during the pitching maneuver and the precise locations of the shed vortices is a strong factor. As with all of these cases, maximizing the power output during any one portion of the flapping cycle may not increase the efficiency of the entire cycle and it is important to do extensive parameter studies to determine the optimum set of flapping parameters for a given flow condition. Still the observation that the decreasing wall distance can increase the plunging power coefficient for some cases is an important one, and the major result of this paper. The effect of the wall distance is more difficult to see in the fast reversal fraction cases ($\Delta T_R = 0.1$) as the large magnitudes of the force and moment coefficients due to the quickly rotating foil obscures the wall contributions. However,

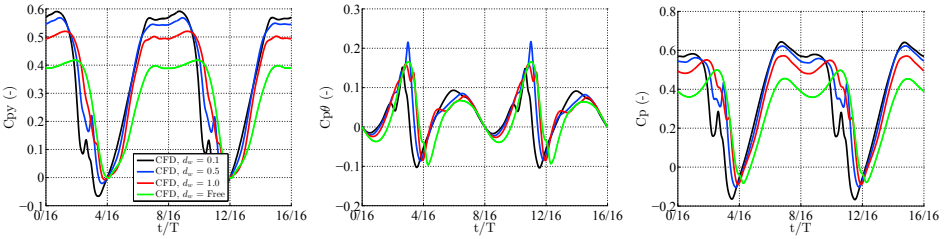

Fig. 4. Power Coefficient Variation as a Function of Wall Distance, $\Delta T_R = 0.5$

some interesting observations are noted, particularly an increase in the lift coefficient when the foil reaches its closest approach to the wall at ($t/T = 4/16$ and $t/T = 12/16$). While this effect is negligible in the overall power extraction efficiency for these cases due to the dominance of the Cp_θ term and the clear unfavorable interaction of the shed vorticity wake during the pitching maneuver, if those issues can be resolved via altering the flapping parameters then the wall effect could be leveraged.

3.3. Comparison with Experimental Results

The experimental results have already been presented in [1], and are only summarized here. The power extraction efficiencies shown in Figure 5 show that the experimental results predict consistently slighly higher efficiencies for all of the reversal fraction cases except the fastest case at $\Delta T_R = 0.1$, where the experimental efficiences are well below the CFD results. However, the trends are similar with respect to the effect of the wall for both the experiment and computational results. Specifically, at the higher reversal fractions the presence of the wall does not increase the efficiency by a discernable amount, but at the slower fractions a small increase in efficiency is exhibited at $d_w = 0.1$ and $d_w = 0.5$. Figure 6 shows the

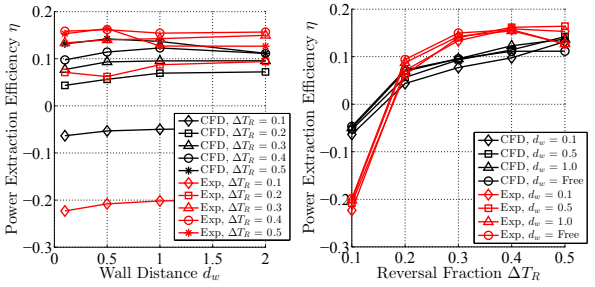

Fig. 5. Power Extraction Efficiency a) As a Function of Wall Distance b) As a Function of Reversal Fraction

vortex pattern comparison for the experimental PIV results and the computational results for portion of the sinusoidal cases at the closest wall distance. The visualiziations are mostly qualitatively simlar, although a few noticble differences can be seen, particularly with the location of the TEV at $t/T = 4/16$, in which the experiment shows the vortex vertically positioned much lower than the computational results indicate. Also, the LEV vortex at $t/T = 7/16$ is positioned on the leeward side of the foil in the experimental results and on the windward side in the computation. More work is needed to understand these discrepancies, but they are likely due to unresolved three dimensional vortex breakdowns such as those demonstrated in higher fidelity three dimensional computational work [9]. Additionally, the flow at these Reynolds numbers is likely quite transitional, and neither the laminar or RANS turbulence models used in this study are adequate to completely accurately capture the complex vortex structure.

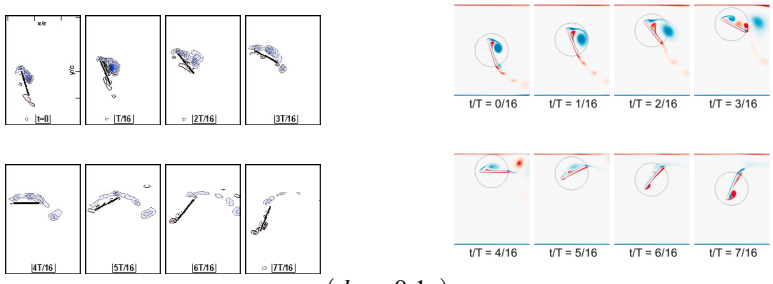

$(d_w = 0.1c)$

Fig. 6. Experimental and Computation vorticity pattern comparison($\Delta T_R = 0.5$, $\phi = 90°$)

4. Conclusions and Future Work

The effect of closely spaced side walls shows some promise in increasing the effect of a flapping foil power extraction system by effectively increasing the lift of the foil during the plunging stroke for certain flow conditions and kinematic parameters. However, this effect is small compared to the effect of the reversal fractions and kinematics of the system, and further study is needed to determine an optimum set of conditions for maximum efficiency. In fact, it is likely that the optimum set of conditions is different for free flow than for constrained flow as the vortex positions vary over the flapping cycle depending on the proximity of the walls.

For future work, much effort could be placed into extensive parameter searches to determine these optimum sets of conditions to maximize the overall efficiency. Additionally, detailed computation studies of the effect of three dimensional vortex breakdown and turbulence modeling effects could help increase our understanding of the problem.

References

[1] F. Karakas, B. Zaloglu, I. Fenercioglu, C. Hoke, J. Young, J. Lai, M. F. Platzer, On Optimal Oscillating-Foil Power Generation in Free and Constrained Flow, AIAA SciTech Forum, American Institute of Aeronautics and Astronautics, 2016. doi:doi:10.2514/6.2016-2070 10.2514/6.2016-2070.

[2] C. M. Hoke, J. Young, J. C. S. Lai, Effects of time-varying camber deformation on flapping foil propulsion and power extraction, Journal of Fluids and Structures Vol. 56 (2015) pp. 152–176. doi:http://dx.doi.org/10.1016/j.jfluidstructs.2015.05.001.

[3] J. Young, M. A. Ashraf, J. C. S. Lai, M. F. Platzer, Numerical simulation of fully passive flapping foil power generation, AIAA Journal Vol. 51 (11) (2013) pp. 2727–2739.

[4] I. Fenercioglu, B. Zaloglu, J. Young, M. Ashraf, J. Lai, M. Platzer, Flow structures around an oscillating-wing power generator, AIAA Journal Vol. 53 (11) (2015) pp. 3316–3326.

[5] M. A. Ashraf, J. Young, J. C. S. Lai, Reynolds number, thickness and camber effects on flapping airfoil propulsion, Journal of Fluids and Structures Vol. 27 (2) (2011) pp. 145–160.

[6] M. Ashraf, A. Isaacs, J. Young, J. Lai, T. Ray, Numerical simulation and multi-objective design of flow over oscillating airfoil for power extraction, in: Conference on Modelling Fluid Flow (CMFF 09), 14th International Conference on Fluid Flow Technologies, Budapest, Hungary, 2009, pp. 9–12.

[7] C. Usoh, J. Young, J. Lai, M. Ashraf, Effective angle of attack control of a flat plate flapping-foil turbine, in: 32nd AIAA Applied Aerodynamics Conference, 2014, p. 3243.

[8] M. F. Platzer, N. Sarigul-Klijn, J. Young, M. Ashraf, J. Lai, Renewable hydrogen production using sailing ships, Journal of Energy Resources Technology Vol. 136 (2) (2014) pp. 021203.

[9] M. R. Visbal, High-fidelity simulation of transitional flows past a plunging airfoil, AIAA Journal Vol. 47 (11) (2009) pp. 2685–2697.